29 October 1965, Volume 150, Number 3696 SCIENCE

Geophysical Observations from Nimbus I

Cloud heights, sea surface, and soil temperatures are mapped from the satellite by infrared radiometry.

William Nordberg

The first photographs of the earth's surface and of large-scale weather systems taken from orbital altitudes have provided a great deal of new knowledge merely because large-scale phenomena which had never been observed in their entirety were now brought within the scope of a single observation. These findings have been obtained from a series of television and infrared observation satellites (Tiros) launched at the rate of about two per year since April 1960. The Tiros satellites were primarily intended to serve the operational needs of the meteorologist in the detection and tracking of storms, frontal systems, and similar phenomena by means of the cloud patterns associated with these weather features. Satellite observations of weather have also contributed to fundamental meteorological research. Nimbus I, the first of NASA's "second generation" meteorological satellites, has further advanced the potential application of such observations to meteorological research and to other fields of geophysics. Various characteristics and components made the Nimbus I system an excellent tool for the remote observation of meteorological and geophysical parameters: a sun-synchronous, nearly polar orbit; a fully earth-oriented, amply powered spacecraft; a set of improved and directly transmitting television cameras; and a newly developed high-resolution infrared radiometer (*1*).

The author is a member of the Laboratory for Atmospheric and Biological Sciences of NASA's Goddard Space Flight Center, Greenbelt, Maryland.

The Nimbus I System

Nimbus I was launched into a nearly polar orbit on 28 August 1964 from Vandenberg Air Force Base, California. Because of a launch-vehicle malfunction, an elliptical orbit (perigee, 423 km; apogee, 933 km) was achieved, instead of the planned circular orbit at 900 kilometers. As planned, the orbital plane was inclined to the equator by 98.7 degrees; this caused the precession of the orbit around the center of the earth to be synchronous with the revolution of the earth around the sun. As a consequence the relative orientation between the orbital plane and the sun remained essentially constant during the life of the spacecraft. Since the launch time was chosen such that the earth-sun line lay in the orbital plane, the satellite passed over most areas of the world twice every 24 hours; at about local noon and local midnight. From two stations in the United States, one in North Carolina, the other in Alaska, commands were given the spacecraft, and the stored telemetric and sensory data were read out. Of the 14 to 15 orbits completed in a 24-hour period, 11 were expected to be within readout range of one of the two stations. The eccentricity of the orbit, however, reduced the number of orbits within this range to fewer than ten per day. Nevertheless, daytime and nighttime photographs were obtained over 50 to 75 percent of the world every day.

The entire Nimbus system, including a complex array of about ten spacecraft subsystems (attitude control, power supplies, telemetry, and so on) as well as data transmission and handling facilities on the ground, had been designed to demonstrate that all the information sensed by the spacecraft could be made directly available to the meteorological analyst in a form suitable for immediate application. For about 4 weeks the experiment functioned perfectly: the three-axis, active control system kept the spacecraft axis (sensor axis) oriented toward the center of the earth at all times, generally within less than 1 degree in all three axes; the solar-cell power supply continually delivered an average power of about 300 watts to the spacecraft; the spacecraft's data storage and transmission system processed more than 50 million items of information (data words) per orbit. Pictorial presentations of the observations made either during the daytime hours with television cameras (Fig. 1) or during the night with a high-resolution infrared radiometer (Fig. 2) were generally available at the NASA Nimbus Control Center in Greenbelt, Maryland, within less than 30 minutes after the command for playback of the data was given to the spacecraft. Within these 30 minutes the information recorded in the spacecraft during any previous orbit (approximately, 100 minutes of observation) was transmitted to the command station (in Alaska, for example), recorded there, then transmitted by way of communication circuits to Greenbelt, Maryland, where latitudinal and longitudinal grids were added automatically and where the data were transcribed onto 70-millimeter photographic film. Examples of the resulting film strips are shown in Figs. 1 and 2. The strips permitted detailed analysis of weather and surface phenomena along the entire globe-circling path of the satellite within less than 2 hours after the observations were made. For operational meteorological applications an "automatic picture transmission system" transmitted television observations instantly to about 50 ground stations located all over the globe. These ground stations, inexpensive and simple to construct, were operated by the U.S. Weather Bureau, the meteorological services of the U.S. Armed Forces, foreign weather services, and, in some cases, educational institutions.

Nimbus Sensors

In the past, television cameras had proved to be the most effective instruments for making observations of meteorological features from satellites. Nimbus I carried two types of cameras: (i) a set of three very-high-resolution cameras each with a field of view of about 35 degrees, and (ii) one camera of lower resolution but with a photosensitive surface which retained a latent image long enough for the image to be transmitted directly by way of the automatic transmission system, without intermediate storage on magnetic tape. The resolution obtained with this camera permitted recognition of cloud and terrain features of less than 4-kilometer diameter. The three high-resolution cameras, which form what is known as the "advanced Vidicon camera system," yielded pictures of considerably greater detail. With these, objects of linear dimensions of less than ½ kilometer could be resolved. This resolution was adequate for observing practically all objects of meteorological significance. The Vidicon cameras were arranged side by side in the satellite and thus covered a strip approximately 2000 kilometers wide along the satellite track.

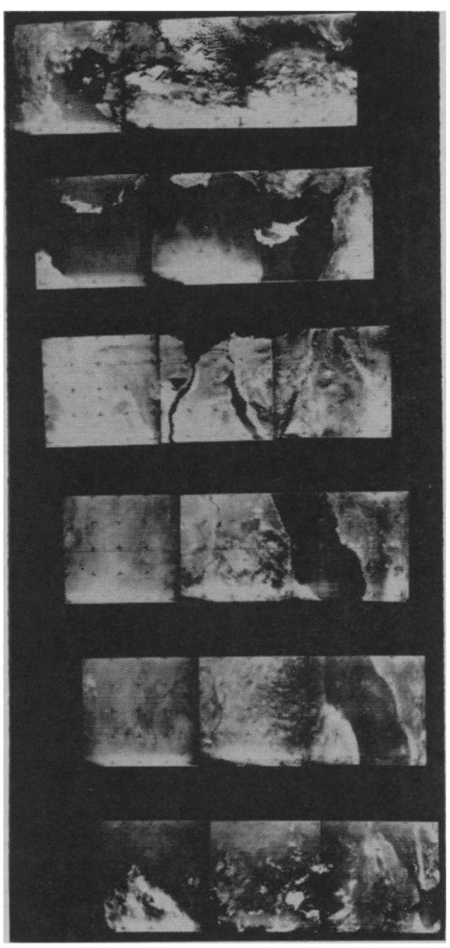

Fig. 1. Pictures made with the "advanced Vidicon camera system" as Nimbus I passed over the Near East at noon on 16 September 1964.

In contrast to the cameras, which formed television images of reflected solar radiation during the day, the high-resolution infrared radiometer provided pictorial presentations, of high quantitative accuracy, of infrared radiation emitted from the earth at night (*2*). The radiation was sensed in the narrow spectral "window" at wavelengths between 3.4 and 4.2 microns. A rotating mirror scanned the earth from horizon to horizon in a direction perpendicular to the orbital path. At each instance during the scan the photodetector measured radiation from a finite area on the surface of the earth. The size of this area, which is a measure of the spatial resolution of the radiometer, varied as the mirror scanned from a point directly below the satellite (the "subsatellite point") toward the horizon. Near the subsatellite point, area sizes range from 3.5 by 3.5 kilometers at perigee to 7.5 by 7.5 kilometers at apogee. At nadir angles of 45°, these areas were about twice as large. The areas measured during one mirror scan formed a band from horizon to horizon along the surface of the earth perpendicular to the orbital path. This band was widest at the horizons and narrowest at the subsatellite point. Due to the motion of the satellite each band lay several kilometers beyond the previous one. Thus, an entire nighttime half of the orbit (Fig. 2) was covered by about 2300 more or less contiguous bands.

The infrared radiometer has been outstandingly successful not only in providing continuous nighttime cover-

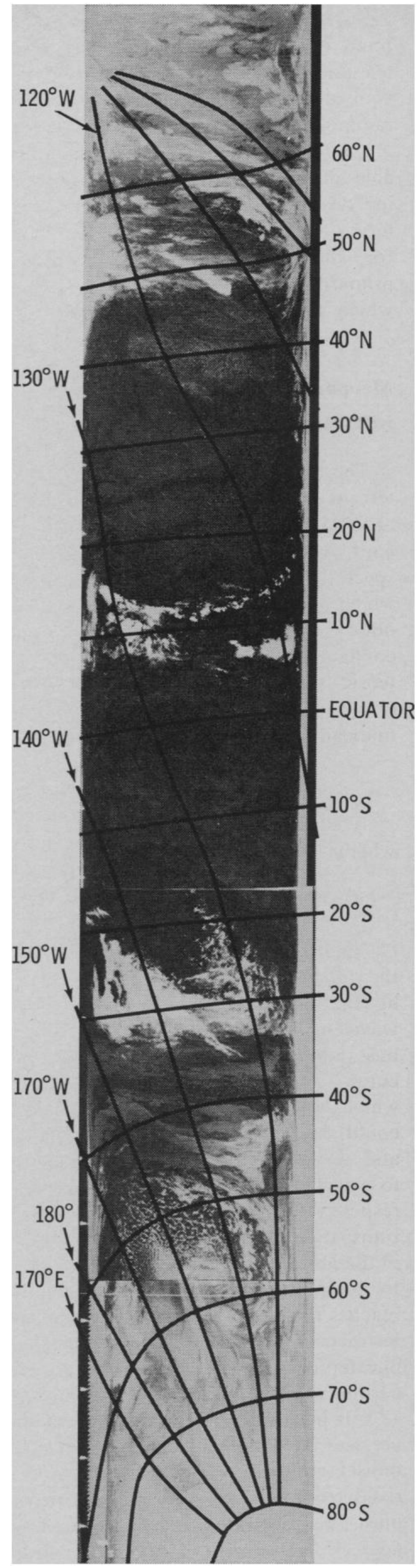

Fig. 2. Radiation picture made with the high-resolution infrared radiometer as Nimbus I passed across North America and the Pacific Ocean from North Pole to South Pole at midnight on 16 September 1964.

age of clouds, with pictorial presentations comparable in quality to Tiros television pictures, but also in resolving equivalent blackbody temperatures of radiating surfaces at night within about $\pm 1°K$. The radiometer was also capable of observing cloud patterns during daylight, but the temperature resolution was lost during daylight hours, for the instrument then responded primarily to reflected solar radiation, which masked the telluric emission.

Mapping Blackbody Temperatures with High-Resolution Radiometery

The principle of mapping cloud and terrain features by means of infrared radiation is quite simple. All objects emit electromagnetic radiation, the spectral distribution and intensity of which are unique functions of the object's temperature (T) and its surface configuration. For blackbodies the intensity is a function of temperature (T_{BB}) only. This fact is expressed mathematically by Planck's law:

$$I_{BB} = \int_{\lambda_1}^{\lambda_2} B(\lambda, T_{BB})\, d\lambda \qquad (1)$$

where

$$B(\lambda, T_{BB}) = (C_1/\lambda^5)\,[\exp C_2/\lambda T - 1]^{-1}$$

C_1 and C_2 are constants, and I_{BB} is the intensity of the radiation emitted by the blackbody surface within the wavelength interval $\lambda_2 - \lambda_1$. The Nimbus radiometer was built to make accurate measurements of I_{BB}, from which surface blackbody temperatures could be inferred. To this end, λ_1 and λ_2 were selected to correspond to wavelengths of 3.4 and 4.2 microns, respectively. The atmosphere is quite transparent in this spectral range. Thus, in the absence of clouds, radiation emitted by the earth's land or water surfaces reaches the satellite with only minor interference by the clear atmosphere. This interference can be corrected for according to computations made by Knude (*3*). If hot (300°K) blackbody surfaces are seen through a tropical (warm and moist) atmosphere, the T_{BB} values derived from the radiation measurements must be corrected by +2 to +4 degrees Kelvin. For a dry atmosphere the correction is somewhat less, and for cold surfaces (<280°K) no correction is necessary. When clouds are present the satellite receives radiation from the uppermost surface of the cloud. When we derive blackbody surface temperatures (T_{BB}) from the measured values of I_{BB} (Eq. 1), we assume that the radiation is emitted isotropically and that the instantaneous field of view of the radiometer is filled by a surface of uniform temperature. The assumption of isotropy is not rigidly valid but must be used for lack of knowledge of the directional variation of I_{BB}. The assumption of uniformity restricts use of the method of deriving surface temperature from radiometer measurements to objects which are homogeneous over a distance of more than about 6 kilometers—for example, cloud formations associated with large-scale meteorological phenomena (fronts, storms, fog layers, and so on) and many terrestrial features, such as deserts, ice caps, and lakes.

Blackbody Temperatures and Surface Temperatures

Equation 1 applies only to blackbodies. Many surfaces, such as water and heavily vegetated, moist areas, are nearly black in this spectral region, and values for T_{BB} derived from Eq. 1 are generally within 2°K of the actual surface temperatures (T). An error of 2°K is commensurate with the error inherent in the measurement of I_{BB}.

Some other surfaces, however, cannot be assumed to be black. Laboratory measurements show that, at wavelengths of about 4 microns, certain minerals and soils may absorb only a fraction (ϵ) of the radiation incident upon their surfaces. Kirchoff's law states that in this case the blackbody emission given by Eq. 1 must be

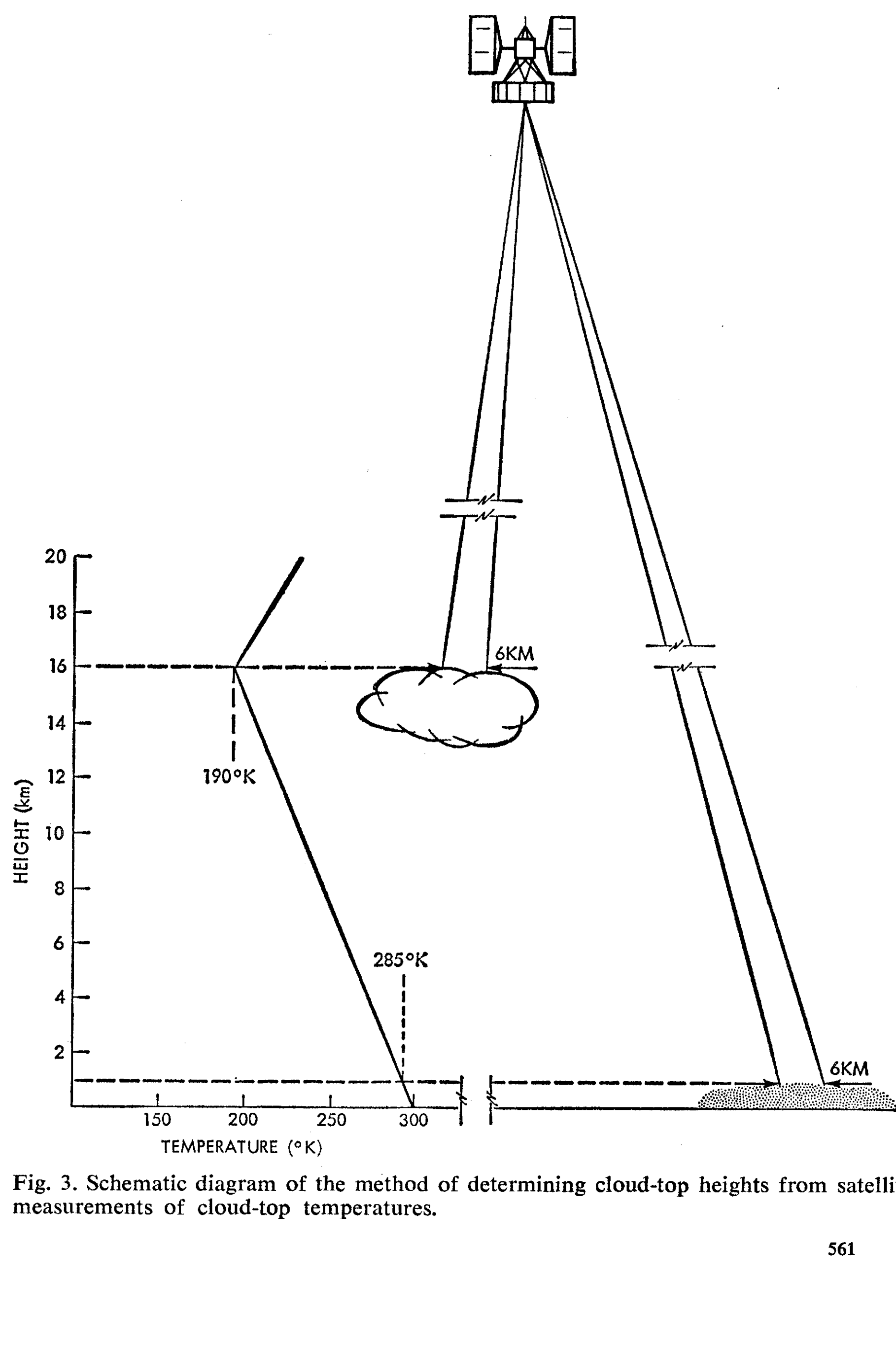

Fig. 3. Schematic diagram of the method of determining cloud-top heights from satellite measurements of cloud-top temperatures.

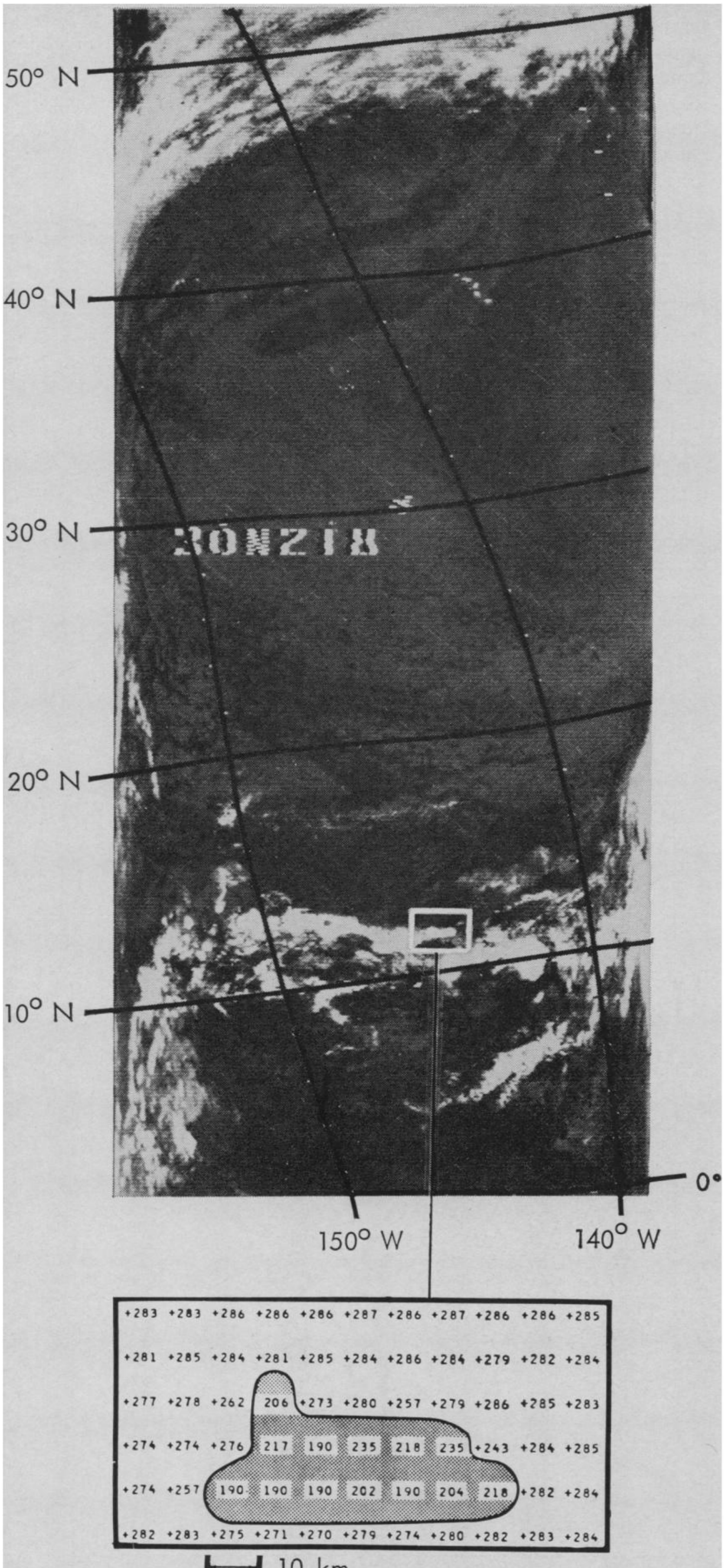

Fig. 4. (Top) Radiation picture of cloud and water temperatures, made from above the North Pacific at midnight on 20 September 1964 (dark tones, warm; white tones, cold). (Bottom) Map, automatically produced by digital computer, of cloud-surface temperatures, corresponding to a small part (framed rectangle) of the picture above.

multiplied by the same fraction ϵ in order to obtain the radiant emittance I_G from a non-black (a gray) body:

$$I_G = \bar{\epsilon} \int_{\lambda_1}^{\lambda_2} B(\lambda, T)\, d\lambda = \bar{\epsilon} I_{BB} \quad (2)$$

The fraction $\bar{\epsilon}$ is the average emissivity of the surface within the wavelength region 3.4 to 4.2 microns.

Using the appropriate values for C_1 and C_2 and for λ_1 and λ_2 in Eq. 1, we find that at a blackbody temperature of 290°K, which is typical for the earth's surface in low-latitude regions, the value of I_{BB} is about 1.4×10^{-1} watt per square meter per steradian. Reduction of this value by 10 percent gives a corresponding T_{BB} value of 288.2°K. This means that a surface of 290°K with an average emissivity of 0.9 emits radiation of the same intensity as a blackbody surface of about 288.2°K. Since the minimum temperature change discernible with the infrared radiometer is about 1° to 2°K, knowledge of $\bar{\epsilon}$ in the derivation of T from I_G is important only if the emissivity is considerably smaller than 0.9.

Surface emissivities can actually be derived from daytime observations of reflected solar radiation. In this case the measured radiation intensities are due not only to surface temperatures but also to the ability of the surfaces to reflect sunlight. The radiation intensity sensed by the radiometer during the daytime I_D is the sum of the emitted gray-body radiation I_G and the reflected solar radiation rI_s. The reflectivity r of practically all terrestrial surfaces is given as: $1 - \epsilon$. Thus, if we define $\bar{r}$ as the average reflectivity in the 3.4- to 4.2-micron range, we may write:

$$I_D = I_G + \bar{r}I_s = \bar{\epsilon}I_{BB} + (1 - \bar{\epsilon})\, I_s \quad (3)$$

I_s is computed from the solar constant on the basis of purely geometrical considerations. A measurement of $I_D = I_s = 1.33$ watt/m^2 per steradian would result if the surface were a perfect, 100-percent-effective, diffuse reflector for solar radiation at vertical incidence. For reflectivity $\bar{r} = 0.5$, emissivity $\bar{\epsilon} = 0.5$, and surface temperature $T = 290$°K, $I_{BB} = 0.07$ and $\bar{r}I_s = 0.7$ watt/m^2 per steradian. Hence, if the surface emissivity is less than 0.5, I_{BB} may be neglected and Eq. 3 reduces to

$$I_D = I_s - \bar{\epsilon}I_s \quad (4)$$

Thus, emissivities can be derived from I_D without any knowledge of surface temperature if $\epsilon < 0.5$ or if $T < 290$°K. For $\bar{\epsilon} > 0.5$, the emissivity can still be measured very accurately provided the surface temperatures are known. For example if $\bar{\epsilon} = 0.99$ and $T = 290°K$, $I_D = 0.15$ watt/m^2 per steradian; if $\bar{\epsilon} = 1.00$ (blackbody), $I_D = 0.14$ watt/m^2 per steradian. The difference of 0.01 watt/m^2 is due to the term $\bar{r}I_s$ in Eq. 3 and its equivalent to a blackbody temperature change of about 2°K, which is just at the sensitivity threshold of the infrared radiometer. In sunlight, emissivities of 0.99 can therefore easily be discerned from blackbodies, and daytime operation of the satellite-borne radiometer provides a very accurate method of measuring large-scale surface emissivities at wavelengths of about 4 microns.

Preliminary evaluations of these daytime observations indicate that emissivities for some large-scale surfaces such as oceans are greater than 0.9. Thus, the infrared-radiometer measurements permit worldwide mapping of actual nighttime temperatures of these surfaces and derivation of emissivities of non-blackbody surfaces from the occasional daytime observations. Global measurements of earth-surface temperatures (as opposed to air temperatures measured near the ground) are of considerable value in meteorological research, since these temperatures relate to the storage of sensible heat at the lower boundary of the atmosphere, an important parameter in the numerical analysis and prediction of weather. At polar latitudes, surface-temperature maps made from radiometer measurements relate to the morphology of ice formations. Such maps are of practical value in navigation and of fundamental interest to glaciologists.

Differences in surface temperatures measured when a satellite is passing over oceans may indicate the locations of currents, fronts, and so on. This suggests potential uses of Nimbus radiometer observations in oceanographic research. The moisture content of soil can be derived at least qualitatively from the Nimbus radiometer observations, since the heat capacity of the soil is increased by moisture and therefore, at night, moist soils are appreciably warmer than dry soils. Aircraft observations, made by Fischer *et al.* (*4*), of emitted infrared radiation over regions of volcanic activity in Hawaii have shown that underground lava beds can be detected with this technique; therefore, use of the Nimbus radiometer data for this purpose was also investigated. No definite identification of active volcanic areas could be made, however, because the spatial resolution of the radiometer is apparently too coarse. Global mapping of emissivity with an instrument of

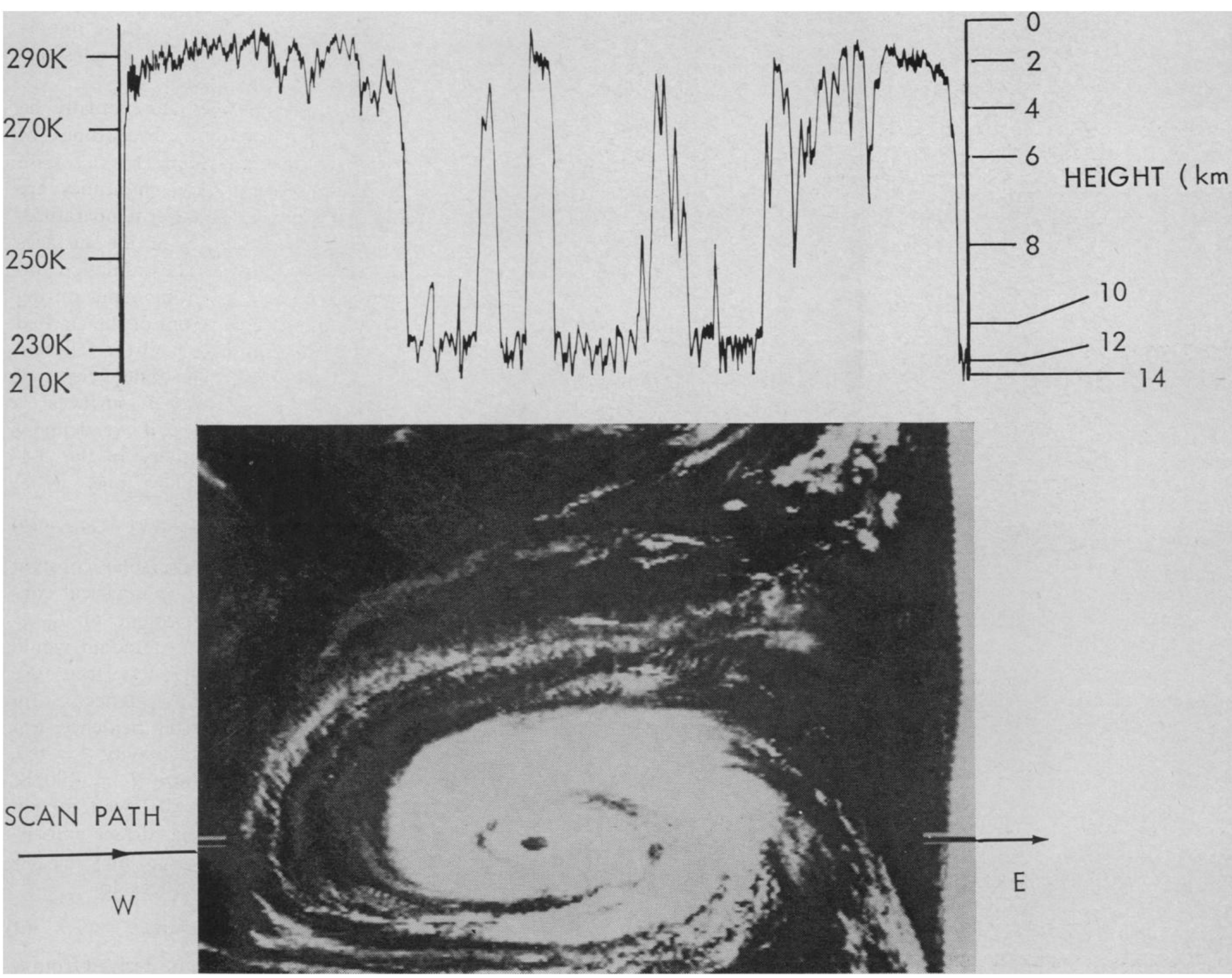

Fig. 5. (Top) Single radiometric scan, from horizon to horizon, across Hurricane Gladys along the scan path indicated in the radiation picture (bottom) of the hurricane; the scan and the picture were made as the satellite passed over the Atlantic at about midnight on 17 September 1964.

such coarse resolution is, nevertheless, of geological interest. Maps of emissivity made from satellite observations might establish a relationship between the small-scale emission properties of various minerals and soil constituents as measured on samples in the laboratory and the large-scale properties of the same constituents in their natural state, where they are blended with impurities and where they vary in grain size, morphology, and so on. The satellite observations should be very useful in determining whether the distribution of mineral and other deposits can be mapped through measurement of emitted radiation with instruments of low spectral and spatial resolution. Any findings in this area may considerably influence the expectations for analogous measurements of lunar and planetary surfaces.

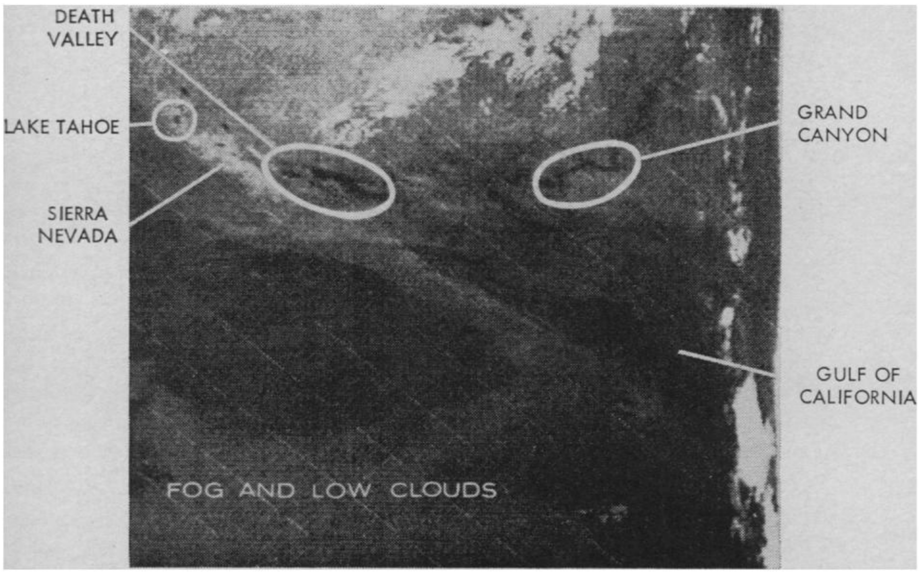

Fig. 6. Radiation picture of ocean and terrain temperatures, made from above the southwestern United States at about midnight on 1 September 1964.

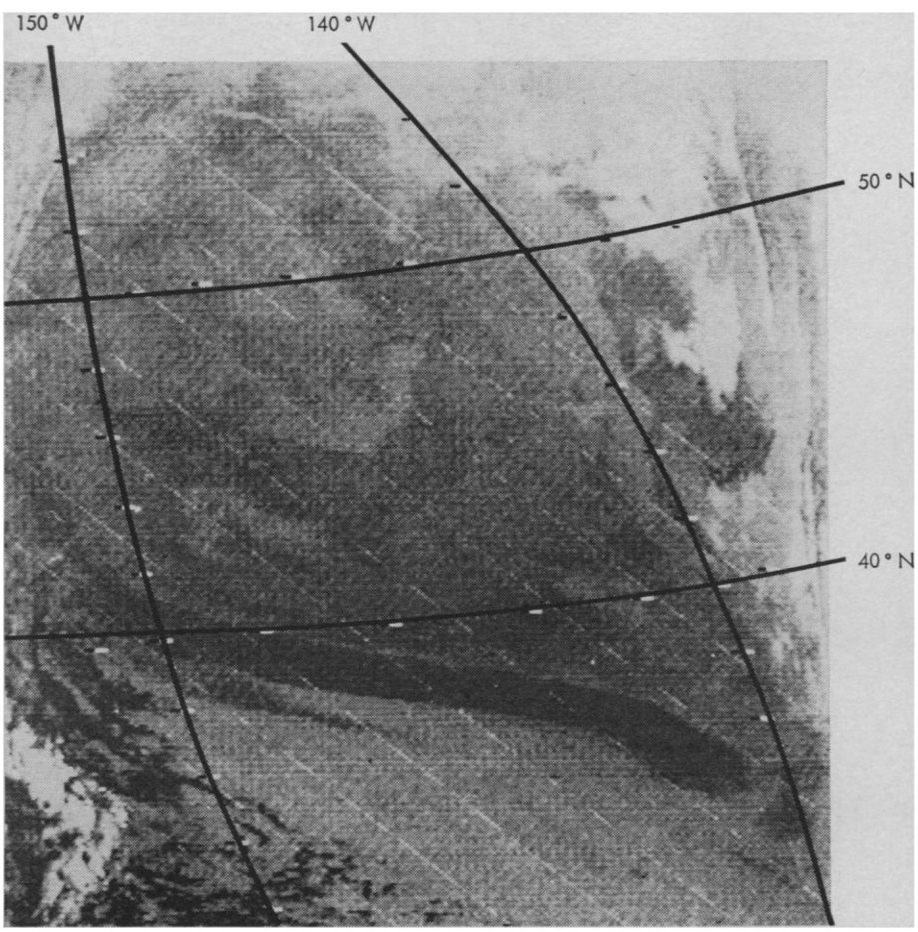

Fig. 7. Radiation picture of cloud and water temperatures, made from above the Pacific Ocean at about midnight on 30 August 1964. A clear streak of open water may be seen in the center of the picture.

Cloud Heights

When the satellite-borne radiometer views a cloud-covered region and a uniform cloud fills the instantaneous field of view of the instrument, the average blackbody temperature of the cloud-top surface can be derived by means of Eq. 1. It is well known that in the troposphere the temperature generally decreases rapidly with altitude. It is also well known that clouds generally do not penetrate to altitudes, above the troposphere, where temperature increases with height. Thus, blackbody temperatures of cloud tops can be directly related to height. (Fig. 3). A deviation of cloud heights from measurements made by satellite-borne radiometers was demonstrated in the case of Tiros observations (*5*); the better spatial resolution of the Nimbus radiometer permits, for the first time, a detailed pictorial presentation of the vertical structure of cloud tops on a large scale. Figure 4 (top) shows a typical example of such cloud structure, over the North Pacific near midnight on 20 September 1964. In this photographic strip, as in all the radiation pictures, high clouds (cold temperatures) appear as light shades of gray, while low clouds or clear areas (warm temperatures) appear dark. Thus, in Fig. 4 (top) the highest clouds are those in the broken cloud band near 10°N; clouds in the broad band near 50°N are somewhat lower, although still much higher than the large mass of clouds (gray) covering the North Pacific from 25° to 45°N. Only a few large, very dark regions, indicating clear skies, can be seen near 40°N, 140°W. The pictorial presentation of these temperature contrasts permits immediate assessment of the gross features of the meteorological situation. The narrow band of very high clouds near the equator marks the Intertropical Convergence Zone; the broad band near 50°N corresponds to an intense cold front, and the dark gray area indicates low-lying fog and stratus clouds stretching south of the front. Of particular interest is the string of small, very bright (cold) spots near 38°–40°N, 137°W. These indicate isolated, very-high-altitude cumulus clouds relating to thunderstorm activity. Normally the meteorologist would never expect thunderstorm activity in the situation then prevailing, especially not near midnight. However, the isolated, very high clouds definitely suggest such activity, and the validity of this interpretation was confirmed by a report from a single ship which happened to be in the area and reported towering cumuli and lightning.

A much more quantitative picture results from automatic plotting of the numerical temperatures, which are derived by digital computer, from the radiation intensities. A part of such a numerical presentation is shown in Fig. 4 (bottom). The very highest cloud in the Intertropical Convergence Zone (11.5°–12°N, 145°–146°W) towers to about 16 kilometers, an altitude derived, by the method of Fig. 3, from the extremely low temperature of 190°K near the center of the cloud top (Fig. 4, bottom). As calculated in this way, the top of the fog near 40°N (Fig. 4, top) had a blackbody temperature of 285°K (this means that it reached only to about 1 km above sea level), and the dark area in the same region had a temperature of about 293°K. The sea-surface temperature as measured by ships in this region was also 293°K, showing that the area was free of clouds. The resolution in the radiometric measurements of cloud heights is vividly demonstrated in Fig. 5 (top), a reproduction of the original analog record of a single scan across the center of Hurricane Gladys made near midnight on 17 September 1964 over the Atlantic. This scan covers a strip 5 kilometers wide, across the storm, and the observed radiation intensities, expressed in equivalent temperatures in degrees Kelvin, are shown on the scale at left. The blackbody temperatures were converted to heights on the basis of actual temperature soundings made by balloons in the vicinity of the storm. These heights are shown on the scale at right. The scan indicates temperatures near 300°K outside the storm and near 290°K in the center of the eye. The temperature of 300°K corresponds to the sea surface temperature in the area of the clear skies outside the storm, and 290°K

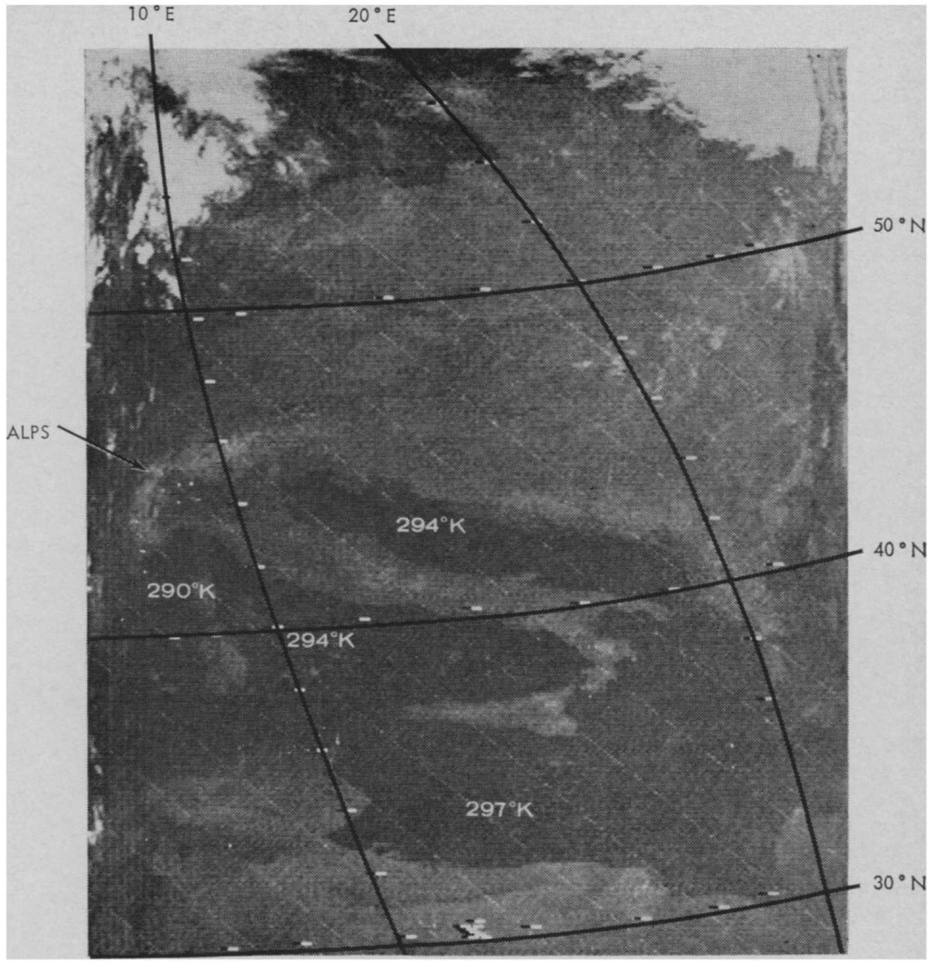

Fig. 8. Radiation picture made from above Europe at about midnight on 14 September 1964.

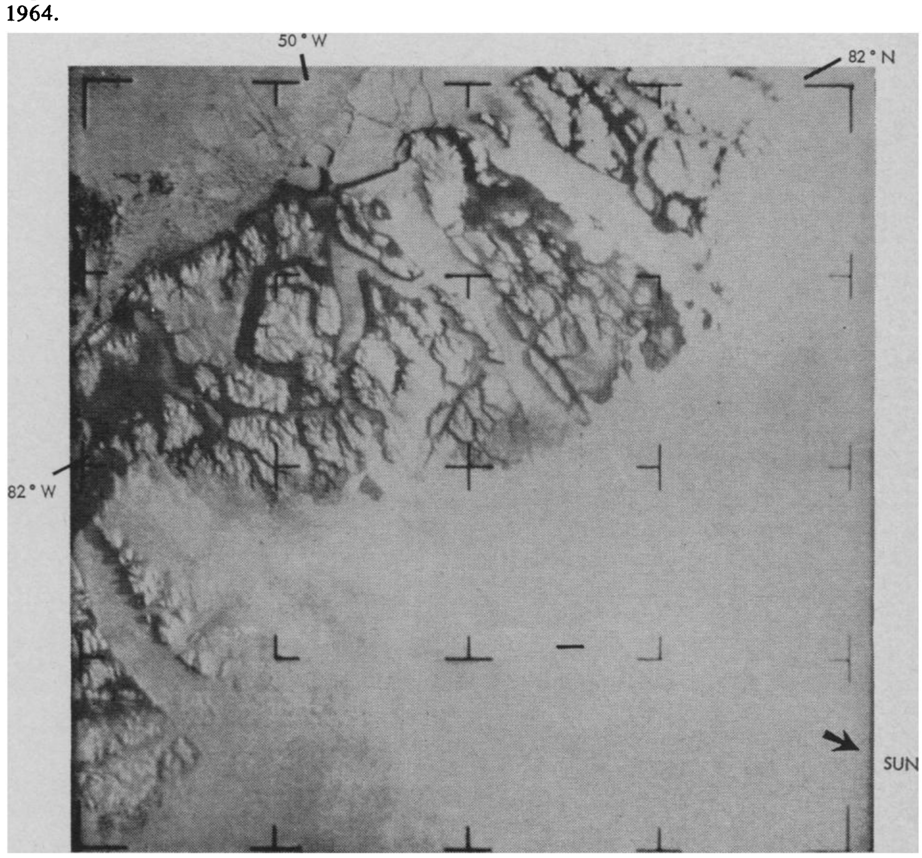

Fig. 9. Picture of northwestern Greenland, taken with the satellite-borne Vidicon camera at about noon on 3 September 1964.

corresponds to a height of 2 kilometers for the tops of clouds inside the eye of the hurricane. Temperatures for the central parts of the spiral bands drop to 200°K, corresponding to heights of 14 kilometers. The scan indicates lower clouds and partially clear skies between the spiral bands. The photographic presentation of the storm (Fig. 5, bottom) is composed from about 200 such scans. These highly quantitative observations of vertical cloud structure in many cases permit a much better exploration of the dynamics of the atmosphere than ordinary cloud photography does. Recently, Samuelson (*6*) has derived emissivities of cloud tops from the Nimbus I daytime radiation measurements (I_D, Eq. 3) and has found that for most types of clouds ϵ ranges near 0.75. This means that for the purpose of deriving absolute cloud heights the T_{BB} measurements must be corrected by approximately $+5°$ to $+10°K$, depending on the cloud temperature and viewing angle, to obtain the true cloud-top temperatures. In general this results in a downward correction of all inferred cloud heights by about 1 kilometer.

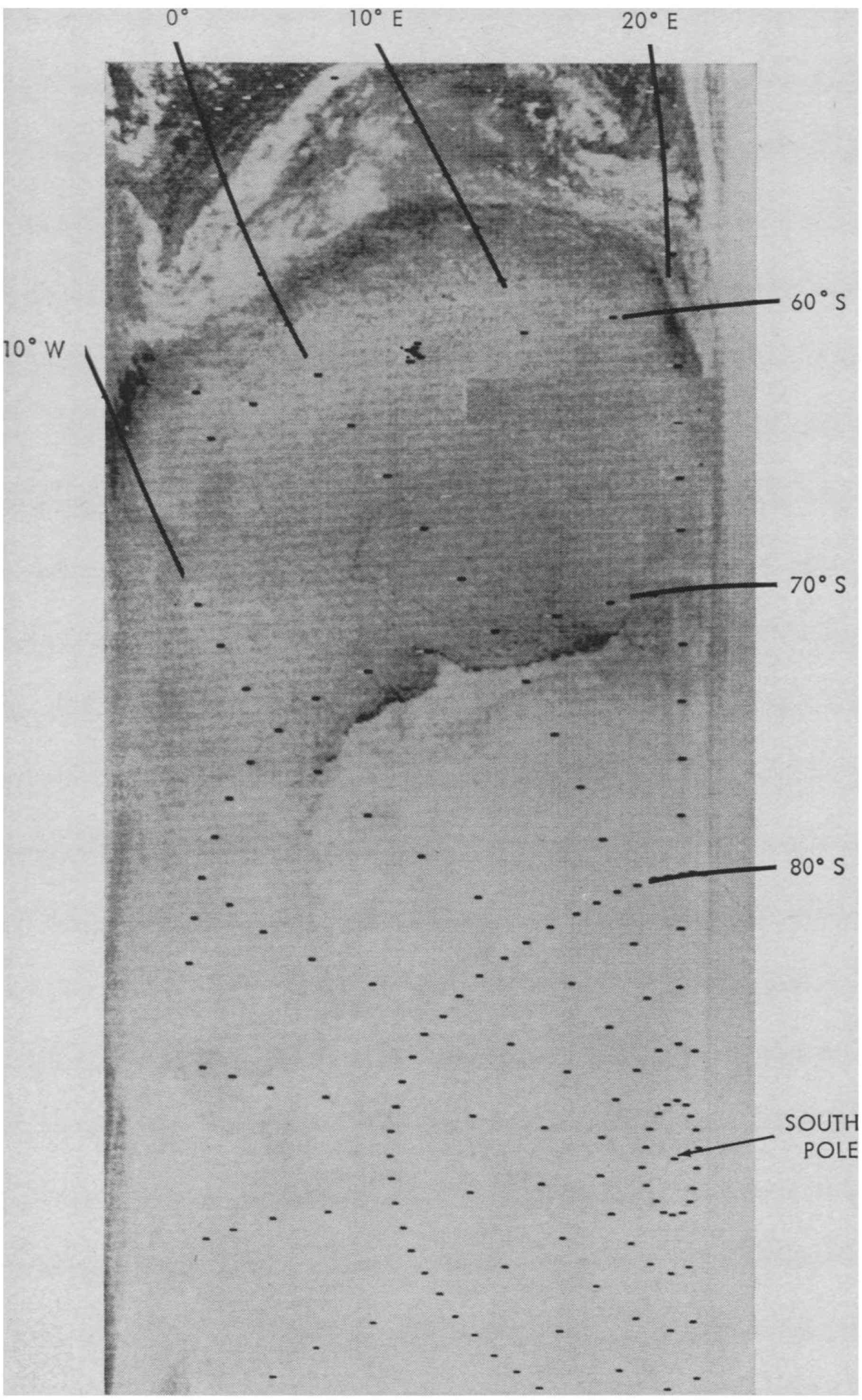

Fig. 10. Radiation picture made from above Antarctica at about midnight on 29 August 1964.

Sea-Surface Temperatures

Since the blackbody assumption for water surfaces is quite valid in the 3.4- to 4.2-micron wavelength range, T_{BB} values derived from the radiation intensities relate directly to water-surface temperatures. Therefore, in cloudless regions the satellite-borne radiometer can be used for global mapping of the surface temperatures of various bodies of water. Figure 6 shows a radiation picture of the southwestern United States at midnight on 30 August 1964. The darkest region (right center) corresponds to a temperature of 301°K for the water surface in the northern Gulf of California. Applying Kunde's corrections for atmospheric absorption (*3*), we obtain a temperature of 303°K for the waters of the Gulf of California, which is considerably warmer than the Pacific Ocean off the shore of California. There temperatures range from 293°K near the coast to about 280°K some 200 kilometers offshore. The low offshore temperatures indicate the presence of fog or dense haze, while the temperature of 293°K measured just west of Los Angeles is in good agreement with the temperatures of 292°K measured from ship board by the U.S. Coast Guard. Even small water features such as lakes can be clearly identified, and their surface temperatures can be determined. The four black (warm) dots in the upper left corner of Fig. 6 are mountain lakes in the Sierra Nevada. The southwesternmost lake is Lake Tahoe. Its water-surface temperature was measured by the radiometer as 283°K, but it is a small body of water, and there is a question whether the field of view of the radiometer was fully covered by the lake. The actual water temperature therefore may have been several degrees higher.

The ability of the radiometer to map sea-surface temperatures suggests that the course of various ocean currents, such as the Gulf Stream, could be detected from the satellite. Unfortunately, during the lifetime of Nimbus I

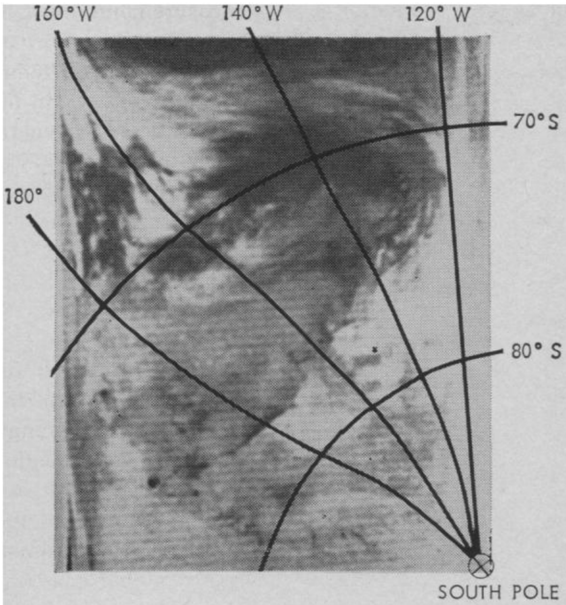

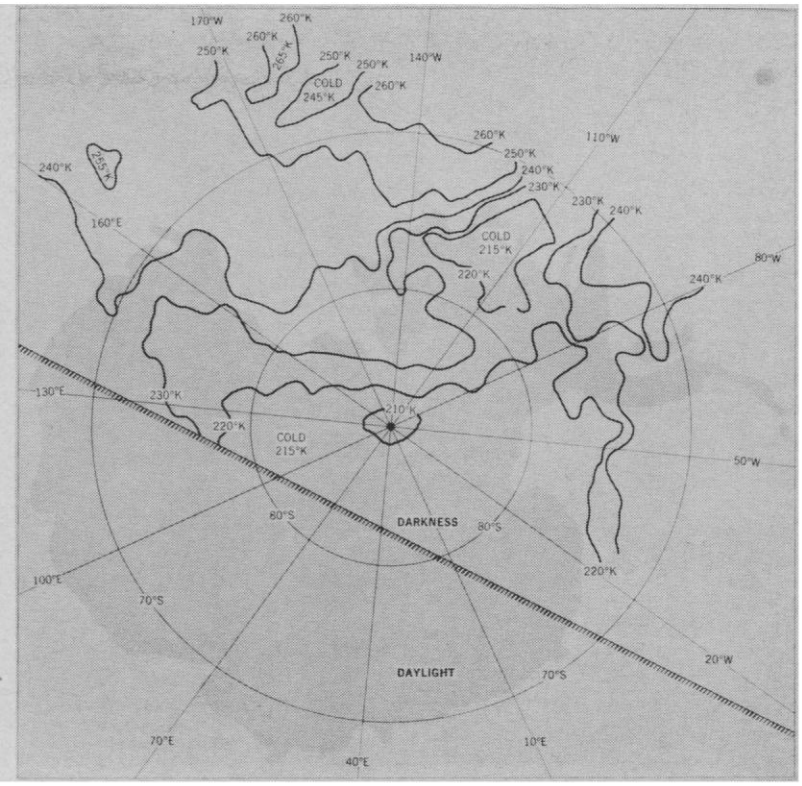

Fig. 11. (Above) Radiation picture made from above Antarctica at about midnight on 1 September 1964. (Right) Map of temperature contours, produced by digital-computer processing of the data presented pictorially at left.

clouds obscured most such areas of interest. There is, however, a possibility that certain cloud formations may themselves be related to ocean temperatures. A suggestion of this can be found in a number of instances for which Fig. 7 is typical. In Fig. 7, clear streaks of open water, very long and narrow, lie between extensive low-altitude stratus-cloud decks over the North Pacific. The streaks are at least 2000 kilometers long and about 200 kilometers wide. Although the phenomenon is apparently atmospheric, it is conceivable that the cloud formations and the peculiar clearings may be influenced by differences in ocean-surface temperature.

Another example of satellite-observed variations in sea-surface temperatures is shown in Fig. 8, a picture obtained when Nimbus I was over the Mediterranean. The derived sea-surface temperatures range from 297°K off the coast of Africa to 290° near Corsica. Temperatures of the Adriatic and Tyrrhenian seas are 294°K.

Ice Formations

Nimbus I was the first weather satellite to provide continuous observations of the polar regions. A great deal of detail in the structure of the inland ice over Antarctica, Greenland, and other areas was observed with the Vidicon camera. High-resolution television observations also provided information on the morphology of floating shelf ice, icebergs, and similar phenomena (*7*). Figure 9, showing the extent of ice cover and the structure of snow-covered mountain ranges over northwestern Greenland, is a typical example of a Vidicon-camera picture. Details in the mountain ranges can be observed because of the pronounced shadows resulting from the low elevation of the sun at these latitudes.

Figure 10 is a radiation picture of temperatures of ice and water surfaces in the Antarctic on 29 August 1964. The entire Atlantic sector of the continent is shown to be cloud-free, and the surface temperatures over the interior ice cap near the South Pole were determined numerically as 210° to 215°K. These extremely low temperatures were observed consistently during the lifetime of Nimbus, from late August to late September. Near the

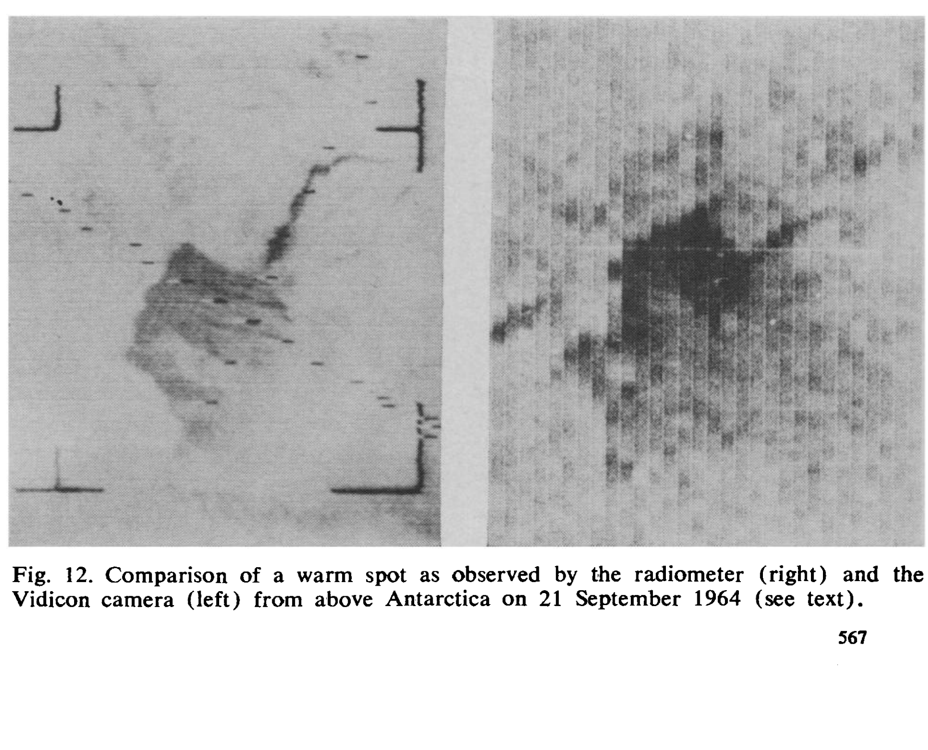

Fig. 12. Comparison of a warm spot as observed by the radiometer (right) and the Vidicon camera (left) from above Antarctica on 21 September 1964 (see text).

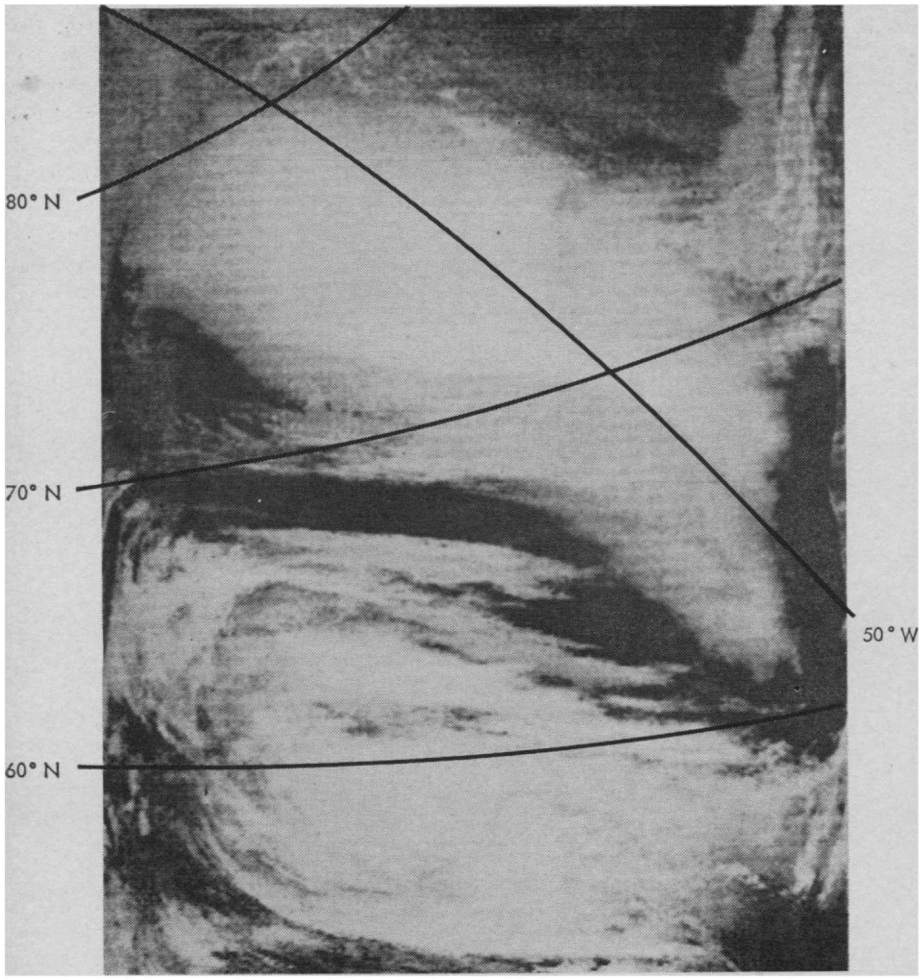

Fig. 13. Radiation picture made from above Greenland at about midnight on 16 September 1964.

edge of the continent surface temperatures increase markedly to about 240°K. The edge of the continent stands out sharply in the infrared picture because a band of apparently open water, in some parts about 100 kilometers wide, stretches along the coast of Queen Maud Land. Maximum temperatures of these areas are about 256°K. This indicates that the full instantaneous field of the radiometer was not viewing an entirely open area of water but that this band probably consists of broken-up ice. A wide shelf of floating ice stretches northward into the Weddell Sea and the Atlantic Ocean. The Weddell Sea ice can be easily distinguished from the inland ice because its surface temperature, 244°K, is about 12° higher than that of the inland sea. Very narrow but distinct lines of warmer temperatures are found crisscrossing the shelf. These lines obviously are due to cracks in the ice, and in some cases they are over 200 kilometers long. The ice shelf extends to 57°S, where it is bounded by open water having temperatures of about 275°K.

Figure 11 (left) is a radiation picture of the Ross Ice Shelf in the Pacific sector of Antarctica. Although these observations were made 4 days after those shown in Fig. 10, the surface temperatures of the inland ice are nearly the same in the two pictures. Surface temperatures of the Ross Ice Shelf range from 225°K, near 85°S, to 245°K, near 70°S. The latter value compares well with the temperatures of 244°K measured 4 days earlier when Nimbus I was over the Weddell Sea (Fig. 10). In Fig. 11 (left) a number of isolated high-temperature spots can be seen along the coast of Victoria Land. The most pronounced one, near 76°S,165°E, has a temperature of 260°K. Since this spot is located near Mount Erebus it was originally suspected that these isolated warm regions might be related to volcanic activity. However, as the same regions were observed in subsequent radiometer pictures it became evident that some of the spots had enlarged and formed small bands along the edge of the continent. Finally, on 21 September 1964 the spot near Mount Erebus had enlarged sufficiently to fill the entire field of view of the radiometer (Fig. 12, right), and the measured temperature was approximately 270°K. The fact that this is conspicuously close to the freezing temperature of water and that the same spot was photographed 12 hours later in sunlight with the Vidicon camera (Fig. 12, left) leads to the conclusion that the spots are indeed open water. Note that the shape of the open area is identical in the two pictures of Fig. 12, despite the difference of one order of magnitude in the resolution capabilities of the Vidicon camera and the radiometer. Figure 11 (right) is a temperature contour map of the Pacific sector of Antarctica, derived from the automatically plotted digital data for the picture shown in Fig. 11 (left). The very low temperatures (215°K) over the high plateau surrounding the South Pole are apparent. The warm tongue reaching toward the pole near 180° longitude coincides with the Ross Sea, where the shelf ice is much warmer than the higher and thicker inland ice. The high clouds seen in Fig. 11 (left) to the east of the Ross Ice Shelf show a temperature of about 215°K, which corresponds to a cloud-top altitude equal to the altitude of the interior plateau—about 3000 meters. The 260°K line indicates pockets of broken ice and open water which are found in the Pacific sector.

A radiation picture of the Greenland ice cap is shown in Fig. 13. Over clear areas the coldest region of the ice mass shows surface temperatures of about 230°K. Cloud bands may be seen extending over the southwest and eastern portion of the subcontinent. Clouds in this case appear darker (warmer) than the underlying ice. The measured cloud temperatures are higher by about 20°K than the ice-surface temperature. This is plausible in view of the temperature "inversions" which are known to exist over the ice-covered polar regions. The term *inversion* means that throughout a portion of the lower atmosphere temperatures *increase* with height, thus deviating from the typical profile shown in Fig. 2. The darkest portions of the region between Greenland and the large cloud mass to the south indicate clear skies over the waters of Baffin

Bay and the Davis Straits. Water-surface temperatures of more than 280°K were derived from digital analysis of the data obtained in observing this area.

Terrain Features and Soil Moisture

Land surfaces are considerably more complex than sea or cloud surfaces. Therefore, under certain conditions, the temperatures derived from radiation intensities measured over land surfaces depend not only on terrain heights but also, to a large extent, on such parameters as heat capacity, conductivity, and moisture content. First, it must be determined whether the variations in radiation intensity are due to differences in actual ground temperatures or to variations in emissivity. In the radiation observations from Nimbus I, most variations may be ascribed to differences in actual surface temperatures. No instances have been found in these observations where variations in surface emissivities could be clearly identified. Indeed, we believe from experience with Nimbus I that effective detection of surface features by means of emissivity measurements from spacecraft will be possible only if the spatial and spectral resolutions of radiometric sensors are improved by several orders of magnitude over the capability of the Nimbus I instruments.

On the other hand, a number of the topographic and geological features mentioned above may be inferred from the measurements of thermal emission in the relatively broad spectral band obtained with the Nimbus I radiometer. For example, the dark streaks in the upper portion of Fig. 6, which shows the southwestern United States, correspond to blackbody temperatures of about 290°K, while the lighter gray in the surrounding regions corresponds to about 275°. The warm streaks were identified as Death Valley and the Grand Canyon. Thus, the temperature differences seen here correspond to differences in terrain height. Furthermore, a more quantitative interpretation of the temperatures over Death Valley reveals that the temperature difference of about 15°K measured by the satellite corresponds to an altitude difference of about 1800 meters between the valley floor and the surrounding highlands. The measured temperature decrease with altitude is therefore about 8.3°K per kilometer—a value in very good agreement with the expected temperature decrease in the free atmosphere (the atmospheric lapse rate). This equilibrium between soil temperatures and atmospheric temperatures leads to the conclusion that the heat capacity of the ground in this area must be generally very large, since only such a large heat capacity will prevent the surface at night from cooling more rapidly by radiation than the overlying atmosphere.

A situation in which considerations other than topographic height changes are involved may be seen in Fig. 14. The picture shows a very large portion of western South America as seen by the radiometer on 14 September 1964, when much of the region was essentially free of clouds; exceptions were the Intertropical Convergence Zone north of 10°S, an extensive low-altitude layer of stratus clouds along the entire west coast, a high-altitude cloud deck off southern Chile, and some smaller clouds along the eastern horizon. The broad, white (cold) band through the center of the picture corresponds to cold, high-altitude mountain ranges of

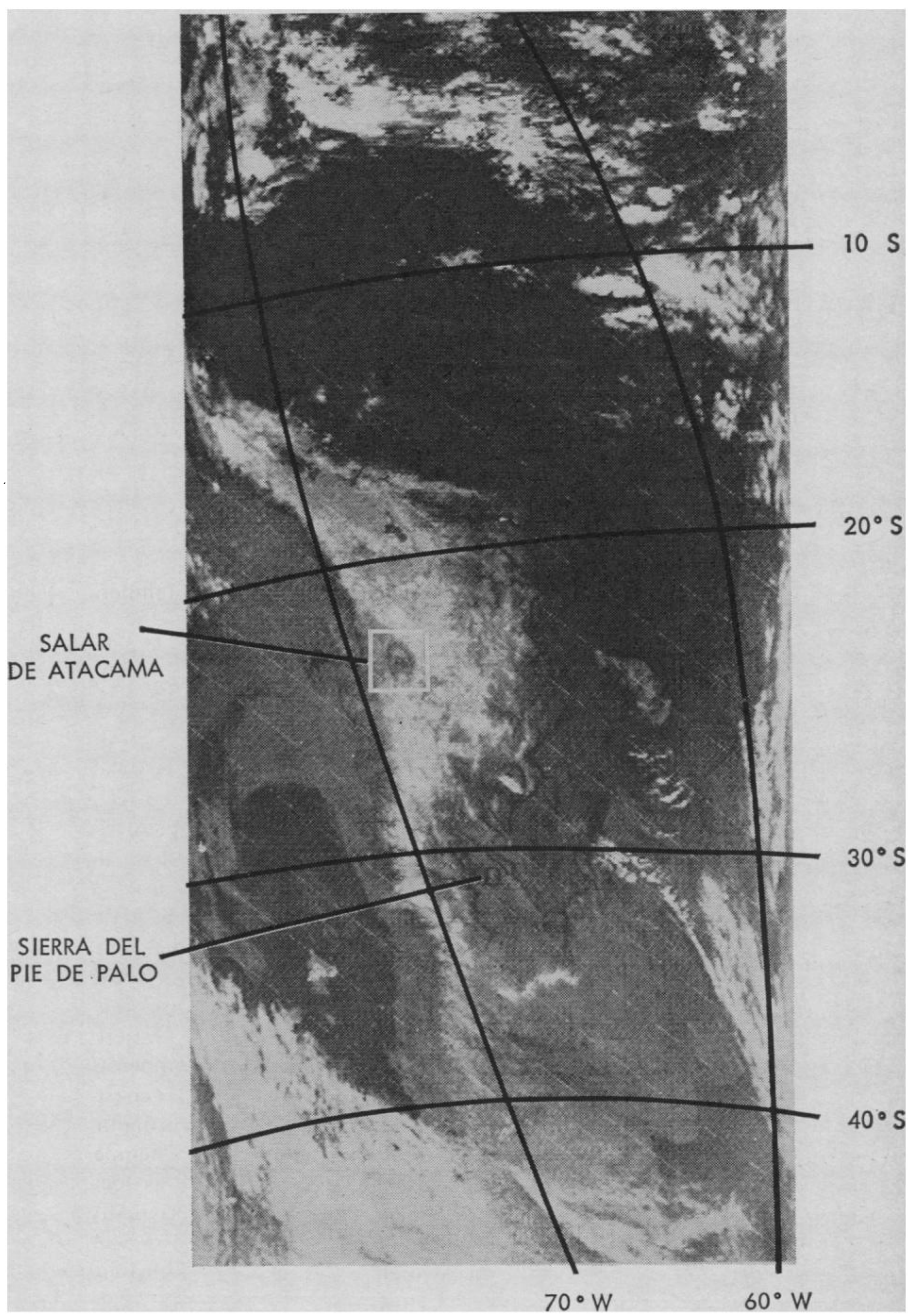

Fig. 14. Radiation picture made from above South America at about midnight on 13 September 1964.

the Andes. Average blackbody temperatures of 255°K are measured over the highest elevations, between 28° and 32°S. To the northeast there is a remarkably rapid transition from the cold highland, with average blackbody temperatures of 270°K, to the very warm Amazon Basin, with blackbody temperatures of 290°K. The warm waters of Lake Poopó (19°S) and Lake Titicaca (16°S) are clearly evident in the generally cold highlands. In the plateaus to the east of the mountains (30° to 35°S) and in northern Chile (24°S) remarkable fine structure in the temperature patterns may be observed. The crescent-shaped form near 23°S corresponds to the Salar de Atacama, a salt flat in northern Chile. The discrete band of warm temperatures (273°K) surrounding the crescent stands out clearly, while the center is quite cold (263°K). The entire Salar has a fairly uniform altitude of about 2300 meters. Thus, on the basis of terrain height, there is no reason to assume the existence of a temperature difference between the center and the rim. Laboratory measurements by Hovis (*8*) have shown that, of many common minerals tested in this spectral region, pure rock salt has the lowest average emissivity, with $\bar{\epsilon} < 0.5$. Therefore, in radiometer measurements pure salt with actual surface temperature of 273°K would give T_{BB} of less than 263°K, while rock formations at the same altitude and temperature (such as those along the periphery of the Salar) would be detected essentially as blackbodies and produce a T_{BB} measurement which was very close to the actual temperature. The difference of 10°K between the cold center and the warm band in Fig. 14 could thus be explained.

It is not certain, however, that the emissivities measured for pure salts in the laboratory are applicable to naturally impure salt deposits such as the Salar. A more probable interpretation is that the emissivity of the natural salt of the Salar is much greater than 0.5 but that the heat capacity of the salt is considerably less than that of the surrounding rock formations at the same altitude level. This difference in heat capacity, together with the very high reflectivity of sunlight and the very low heat conductivity of the deposits of relatively fine grained salt, prevents the storage of large amounts of solar heat in the Salar itself and, after sunset, causes it to cool very rapidly by radiation, a process which results in a very low temperature (263°K) at midnight. The rocks along the periphery, however, remain warmer (273°K) throughout the night, because of their larger heat capacity and greater conductivity.

A similar situation may be seen in Fig. 14 near 32°S,68°W, part of western Argentina as seen by the radiometer. Here, a nearly circular dark band about 5 kilometers wide and 40 to 50 kilometers in diameter indicates the existence of a high-temperature zone. The cold temperatures (light spot) in the center of the band can be easily explained by topography. The center of the band corresponds to the Pie de Palo mountains, shown topographically in Fig. 15. The lowest temperature measured in the center of the band is 268°K and corresponds to the highest elevation, about 3000 meters (Fig. 15). The temperature along the band is about 280°K—about 7° higher than the temperature of the surrounding desert. Since the band around the mountain is certainly not at a lower altitude than the surrounding desert plateau (Fig. 15), the explanation of the warmer temperatures must be found in the difference in heat storage between the desert sand and the rocks of the Pie de Palo mountains. A visual survey (*9*) revealed that the contrast between the Precambrian rock formations of the Pie de Palo mountains and the alluvial sand deposits of the surrounding desert is indeed very striking and occurs around the mountains approximately along the 1000-meter con-

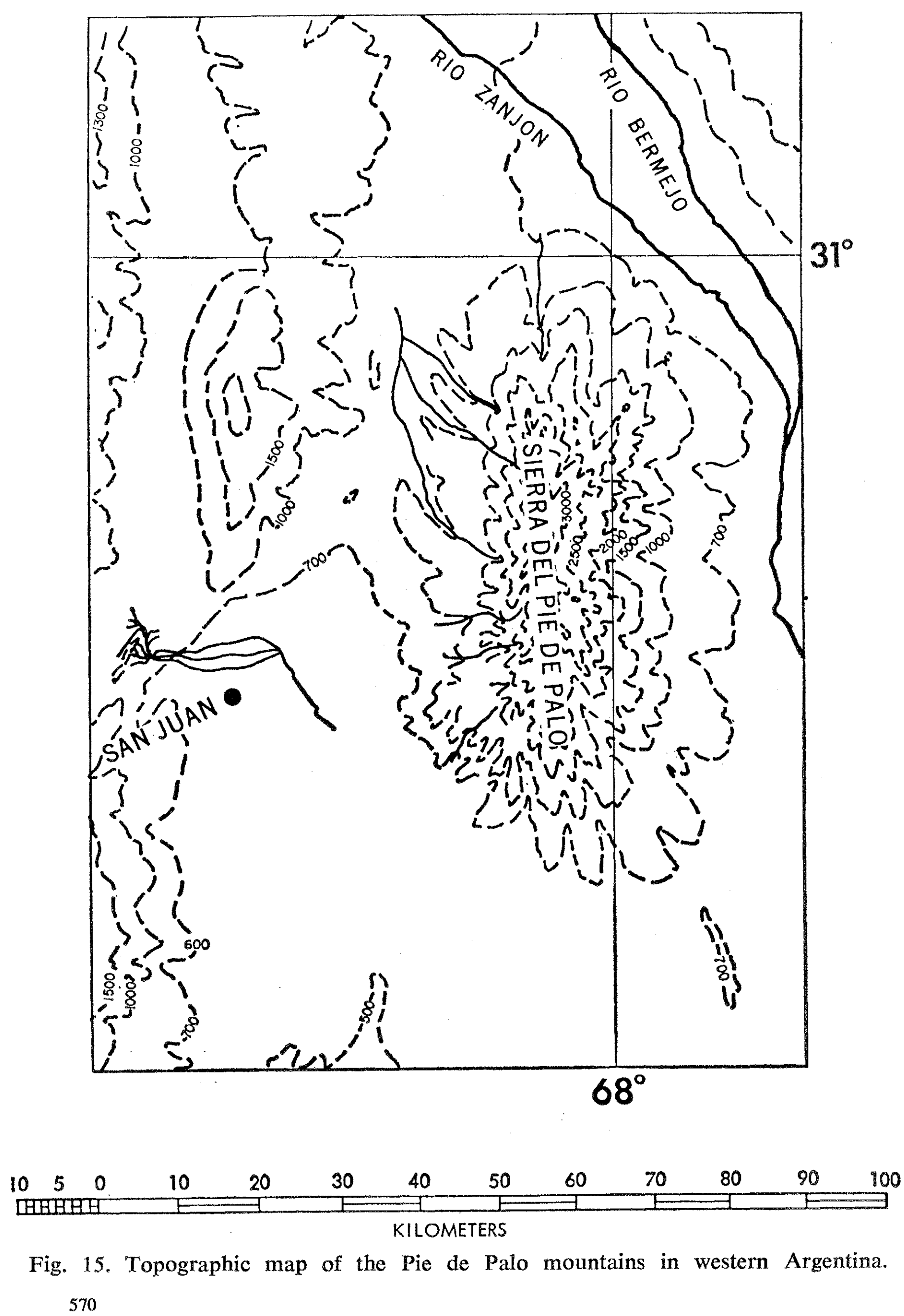

Fig. 15. Topographic map of the Pie de Palo mountains in western Argentina.

tour line (Fig. 15). The dark band seen by the satellite approximately parallels this 1000-meter contour line. Furthermore, the temperature difference of 12°K between the warm band at 1000 meters and the cold top of the mountain, which rises abruptly to 3000 meters, yields an approximate lapse rate of 6°K per kilometer. This corresponds to the expected adiabatic lapse rate much more closely than the temperature difference of 6° between the desert plateau at about 800 meters and the mountain top does. That latter difference would yield a rather unrealistic lapse rate of 3°K per kilometer. Thus, the temperature of the desert at night is considerably lower than the air temperature because of the small heat capacity and low conductivity of the ground. This low soil temperature results in a temperature inversion in the air over the desert, while the solid rocks remain considerably warmer, resulting in the adiabatically decreasing temperature from the periphery to the center of the mountain.

Pictures obtained as the satellite passed over the deserts of North Africa and the Near East exhibit similar fine structure in the emitted radiation; this fine structure implies temperature variations of 10° to 15°K. Again, we conclude that these gradients are due to variations in the thermal properties of the soil rather than variations in emissivity.

Thus, the small-scale radiometer observations permit the mapping of geological features which can be distinguished by their thermal properties. On a larger scale these patterns of heat capacity are of meteorological significance, since storage of heat in the ground is an important consideration in the numerical description of atmospheric processes.

The moisture content of the soil is also evident in the radiometer observations. It has been very surprising to find that many rivers less than 1 kilometer wide stand out prominently in the radiation pictures even though the linear resolution of the instrument is generally no better than 5 kilometers. The prominence of the rivers is apparently due to the fact that the heat capacity of the ground along these rivers has been altered, probably by moisture in the ground, the moist ground retaining solar heat absorbed during the daytime much longer than the adjacent drier regions do. In Fig. 14, several rivers may be seen to the east of the Andes. Two of them are particularly prominent; their confluence is just to the east of the conspicuous warm band around the Pie de Palo mountains. They can be identified as the Rio Zanjón and the Rio Bermejo in northwestern Argentina. Interestingly, despite their prominence in the radiation pictures, these rivers are less than a few hundred meters wide and, except for occasional spring flooding, carry almost no water. Moreover, they do not form any deep canyons or other depressions in this area, so their warmer temperatures cannot be explained by differences in height. The explanation must be that, in times past, these rivers spread to widths of several kilometers and meandered over the desert plateau. These meanderings apparently took place during the flood stages, and they must have altered the terrain sufficiently to produce a contrast in the thermal properties between the desert and the river beds, hence nighttime temperature differences which were detected by the satellite radiometer. Of course, such contrasts can only be produced where the surrounding terrain is very dry and its heat capacity very small. For example, in Fig. 14 only vague indications can be found of the Amazon River, which is much wider than the Bermejo and Zanjón rivers, which stand out so clearly. The entire Amazon Basin has such a large heat capacity, due to its moisture and heavy

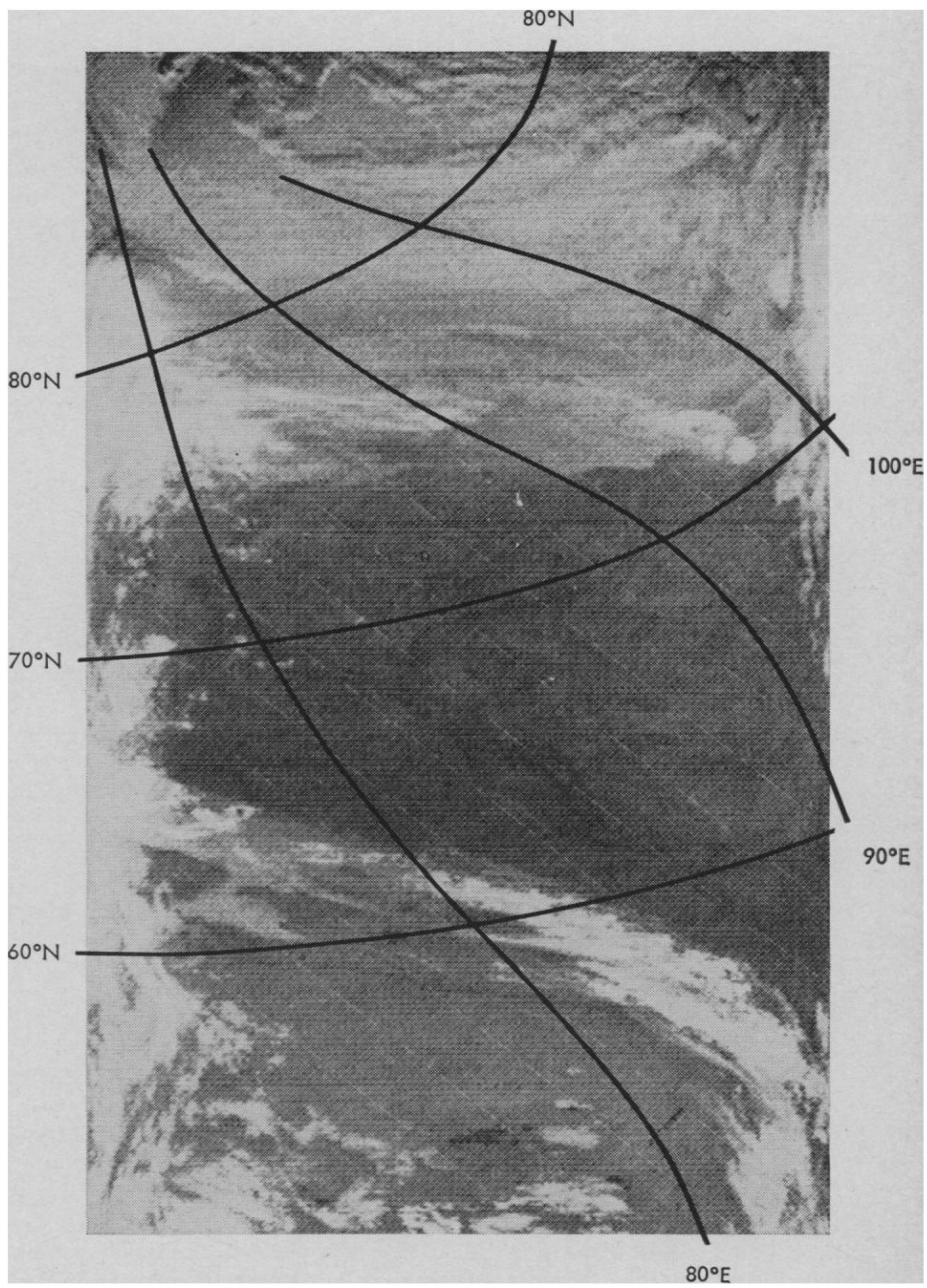

Fig. 16. Radiation picture made from above Siberia at midnight on 5 September 1964.

vegetation, that a uniform and high temperature is maintained throughout the night. Because of this fact, in the radiometric observations of tropical regions the boundaries between water and land, hence parts of the outlines of continents, cannot be distinguished.

Comparison of a radiation picture of the Siberian tundra on 5 September 1964 (Fig. 16) and hydrometeorological data for the same date provides an example of very close equilibrium between soil and air temperatures. In Fig. 16 a band of clouds, indicating a cold front, lies across western Siberia near 60°N. The skies to the north and south are cloudless; this is indicated by the clearly visible lakes and rivers on both sides of the front. Blackbody temperatures, however, are markedly different on the two sides. To the south of the front the temperatures range from 277° to about 280°K, while to the northwest they are about 287°. Surface-air data provided by the Hydrometeorological Service of the U.S.S.R. show that surface-air temperatures in the southern region were about 279°K, while in the northwest they ranged from 283° to 288°K. This agreement with the satellite-measured soil temperatures suggests a complete equilibrium between air and soil temperatures in this region. Other radiometer observations were obtained when the satellite passed over this area during September 1964, but the north-south temperature contrast was apparent only on 5 September. This leads to the rather surprising conclusion that, in this case, the soil temperatures were governed by the temperatures of the overlying air masses.

Thus, a variety of geophysical and atmospheric facts can be inferred from the satellite observations of temperature variations over clouds, oceans, ice formations, and the earth's terrain. The height distribution of the tops of clouds can be determined from the temperatures of cloud surfaces. Temperature measurements of the surfaces of oceans and extensive vegetated regions are of great importance to meteorology. The heat capacities of these regions are so large that the ground (or water) acts as a reservoir which heats or cools (depending on its own temperature) the air moving over it.

In dry, sandy terrain, the heat capacity of the ground is so small that, at night, when there is no solar radiation, the ground temperatures are very low, generally much lower than air temperatures. In more solid, rocky surfaces and in moist terrain, surface temperatures remain high during the night, generally the same as air temperatures. Thus, contrasts in the thermal properties of the surfaces usually produce a pronounced fine structure in the radiation picture. In many cases, these contrasts can be interpreted, qualitatively at least, as a measure of the moisture content of the ground or a measure of changes in vegetation or geological formation (*10*).

References and Notes

1. W. Nordberg and H. Press, *Bull. Am. Meteorol. Soc.* **45**, 684 (1964).
2. I. L. Goldberg, L. Foshee, W. Nordberg, C. Catoe, *Proc. Symp. Remote Sensing of Environment, 3rd, Univ. Mich.* (1965), pp. 141-51.
3. V. G. Kunde, in "Meteorological and Geophysical Observations with the NIMBUS I Satellite," *NASA (Natl. Aeron. Space Admin.) Spec. Publ.*, in press.
4. W. A. Fischer, R. M. Moxham, F. Polcyn, G. H. Landis, *Science* **146**, 733 (1964).
5. W. R. Bandeen, V. Kunde, W. Nordberg, H. Thompson, *Tellus* **16**, 481 (1964); L. J. Allison and G. Warnecke, in "A Quasi Global Presentation of TIROS III Data," *NASA (Natl. Aeron. Space Admin.) Spec. Publ 53* (1964).
6. R. E. Samuelson, "Reflectances and emissivities of Clouds in the 3.5-4.1 micron infrared window as determined from the Nimbus I meteorological satellite," in preparation.
7. R. Popham and R. E. Samuelson, in "Meteorological and Geophysical Observations with the NIMBUS I Satellite," *NASA (Natl. Aeron. Space Admin.) Spec. Publ.*, in press.
8. W. Hovis, *J. Appl. Optics*, in press.
9. The survey was made possible by the staff of the University of San Juan, San Juan, Argentina. I am especially indebted to Professor C. V. Cesco, who provided me with valuable background material for this investigation.
10. The observational data discussed are available for further analysis by the scientific community: a catalog of all Nimbus radiometer observations is given in *NIMBUS I High Resolution Radiation Data Catalog and Users Manual* (Goddard Space Flight Center, Greenbelt, Md., 1965), vol. 1.

Computer-Aided Instruction

Concepts and problem-solving techniques can be learned by conversing with a programmed-computer system.

John A. Swets and Wallace Feurzeig

Computers as teaching machines can present lesson materials, and accept student responses, in several forms. A computer can type on an electric typewriter, generate text and pictures on a television screen, and control a slide projector and tape recorder; the student can type, write with a "light pen" on the television screen, or respond by means of some special device. The computer-based teaching machine can keep various scores, and use them to select an appropriate path through a lesson for any particular student. A time-shared computer serves many users simultaneously, so that complicated decisions can be made for each student at low cost. The computer can keep records of student progress, with summary statistics for individuals and groups, and produce them on call. This kind of teaching machine can act like any one of a number of fixed machines. Given the necessary preparations, the stimulus and response modes and the lesson content can be readily changed.

These capabilities are at present exercised in a half-dozen or so prototype, programmed-computer systems. The report of a recent conference (*1*) is a convenient reference.

This article describes a system for instruction that uses the power of the computer in other ways, in an attempt to deal more effectively with complex subject matters. The system was designed for use with rich materials that may be expected to suffer when they are reduced to machine-controlled step-by-step presentation of small pieces of information and associated questions requiring short answers from the student.

The authors are associated with Bolt Beranek and Newman Inc., Cambridge, Massachusetts.